Active Phase Separation (in two dimensions)

Leticia F. Cugliandolo

Sorbonne Université

Institut Universitaire de France

leticia@lpthe.jussieu.fr
www.lpthe.jussieu.fr/˜leticia

Work in collaboration with

C. Caporusso, **G. Gonnella**, **P. Digregorio & I. Petrelli** (Bari, Italia)

A. Suma (Trieste, Italia, Philadelphia, USA & Bari, Italia)

D. Levis & I. Pagonabarraga (Barcelona, España & Lausanne, Suisse)

Cambridge 2022

Active Brownian Disks in $2d$

(Overdamped) Langevin equations (the standard model)

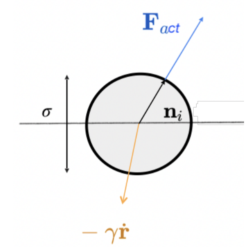

Active force $\mathbf{F}_{\rm act}$ along $\mathbf{n}_i = (\cos\theta_i, \sin\theta_i)$

$$m\ddot{\mathbf{r}}_i + \gamma\dot{\mathbf{r}}_i = F_{\rm act}\mathbf{n}_i - \nabla_i \sum_{j(\neq i)} U_{\rm Mie}(r_{ij}) + \boldsymbol{\xi}_i \;, \qquad \dot{\theta}_i = \eta_i \;,$$

$\mathbf{r}_i$ position of ith particle & $r_{ij} = |\mathbf{r}_i - \mathbf{r}_j|$ inter-part distance,

$U_{\rm Mie}$ short-range **repulsive** Mie potential, over-damped limit $m \ll \gamma$

$\boldsymbol{\xi}$ and η zero-mean Gaussian noises with

$\langle \xi_i^a(t)\, \xi_j^b(t')\rangle = 2\gamma k_BT\delta_{ij}^{ab}\delta(t-t')$ and $\langle \eta_i(t)\, \eta_j(t')\rangle = 2D_\theta\delta_{ij}\delta(t-t')$

The units of length, time and energy are given by σ, $\tau_p = D_\theta^{-1}$ and ε

$D_\theta = 3k_BT/(\gamma\sigma^2)$ controls persistence, $\gamma/m = 10$ and $k_BT = 0.05$

Péclet number Pe = $F_{\rm act}\sigma/(k_BT)$ and $\phi = \pi\sigma^2 N/(4S)$, measures activity

Active Brownian disks

The typical motion of particles in interaction

Passive

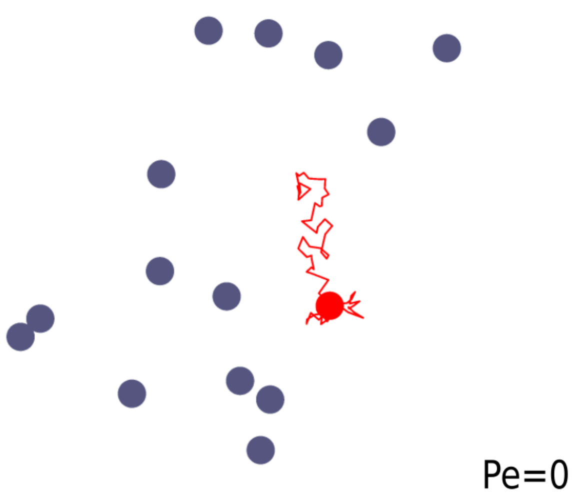

Active

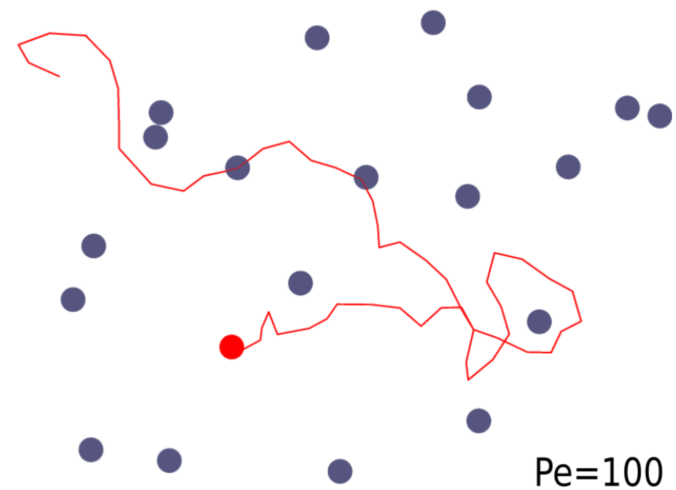

The active force induces a **persistent random motion** due to

$$\langle \mathbf{F}_{\rm act}(t) \cdot \mathbf{F}_{\rm act}(t') \rangle \propto F_{\rm act}^2 \, e^{-(t-t')/\tau_p}$$

with $\tau_p = D_\theta^{-1} \sim 60$

Active Brownian disks

Phase diagram with solid, hexatic, liquid, co-existence and MIPS

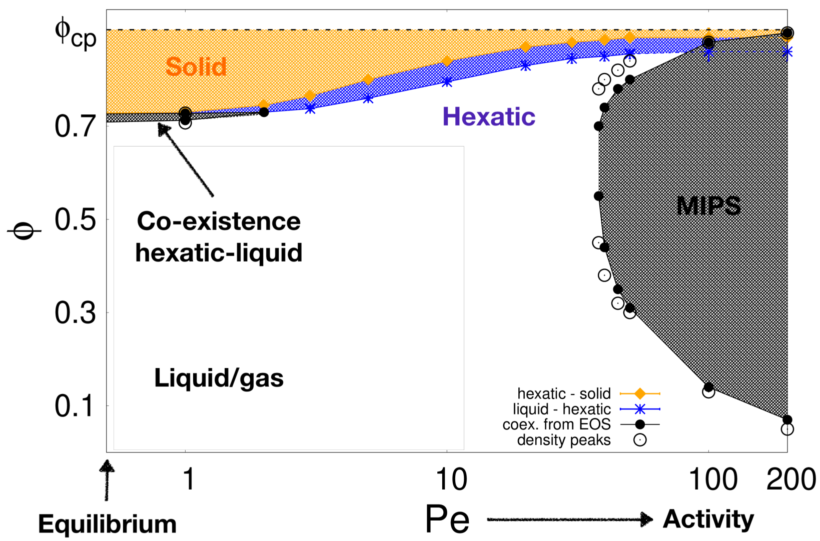

1st order **hexatic**-**liquid** close to Pe = 0

KT-HNY **solid**-**hexatic**

- universal dislocation unbinding

Breakdown of KT-HNY **hexatic**-**liquid** picture

- disclination unbinding within the **liquid** phase

- **percolation** of defect clusters in the liquid

Pressure $P(\phi, \mathrm{Pe})$ (EoS), correlations $G_T(r)$, $G_6(r)$, distributions of ϕ_i, and $|\psi_{6i}|$, defect identification & their densities

Digregorio, Levis, Suma, LFC, Gonnella & Pagonabarraga, PRL 121, 098003 (2018)

Digregorio, Levis, LFC, Gonnella & Pagonabarraga, Soft Matter 18, 566 (2022)

Active Brownian disks

Phase diagram with solid, hexatic, liquid, co-existence and MIPS

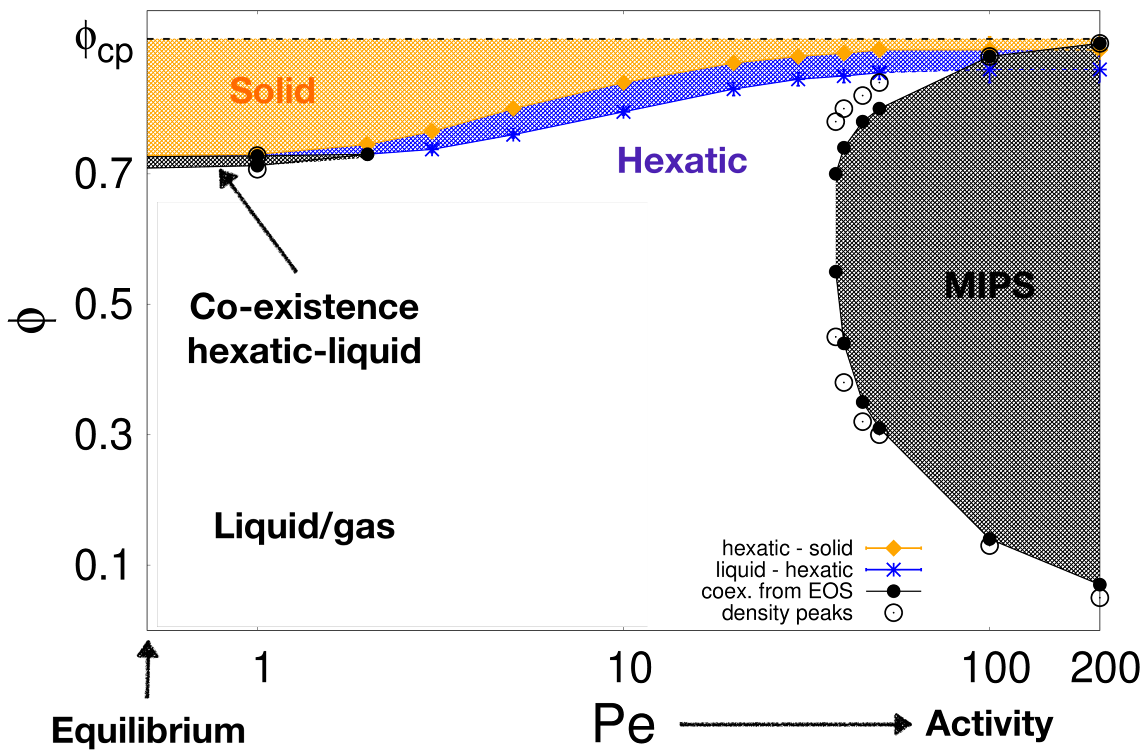

Motility induced

phase separation (MIPS)

gas & dense

Cates & Tailleur
Ann. Rev. CM 6, 219 (2015)
Farage, Krinninger & Brader
PRE 91, 042310 (2015)

Pressure $P(\phi, \mathrm{Pe})$ (EOS), correlations $G_T(r)$, $G_6(r)$, and distributions of ϕ_i, $|\psi_{6i}|$

Digregorio, Levis, Suma, LFC, Gonnella & Pagonabarraga, PRL 121, 098003 (2018)

Motility Induced Phase Separation

The basic mechanism

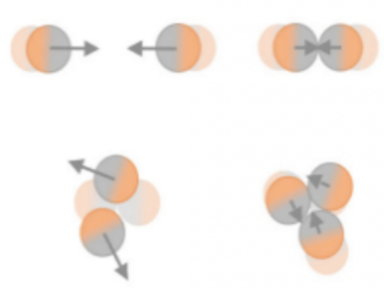

Particles collide heads-on

and cluster even in the

absence of attractive forces

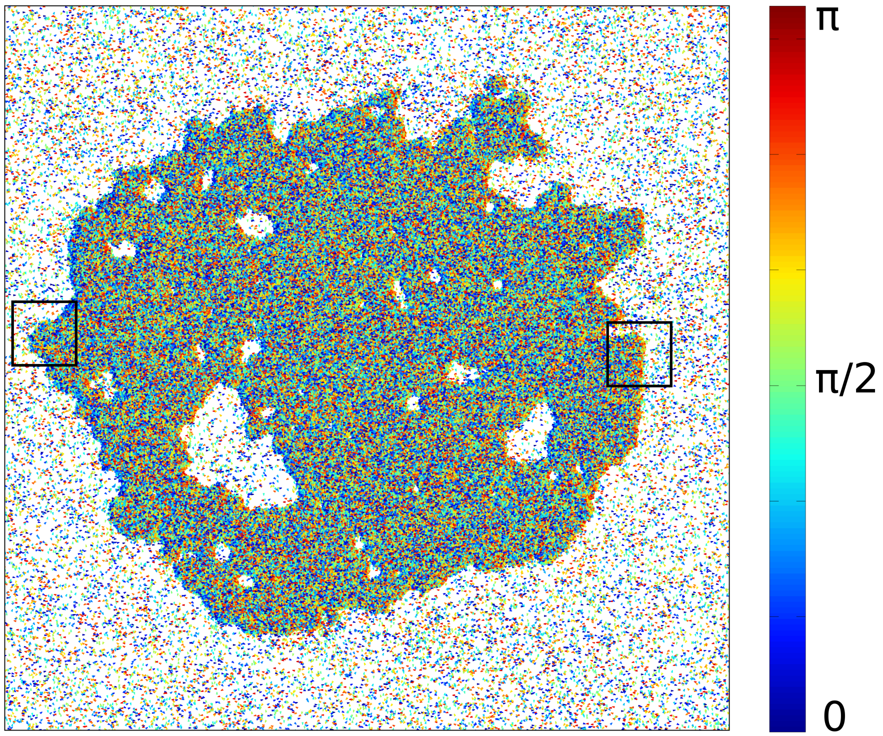

$\longrightarrow$ **blue 0** $\longleftarrow$ **red π**

The colours indicate the direction along which the particles are pushed by the active force $\boldsymbol{F}_{\rm act}$

The dense phase

Hexatic patches, defects & interfaces, bubbles

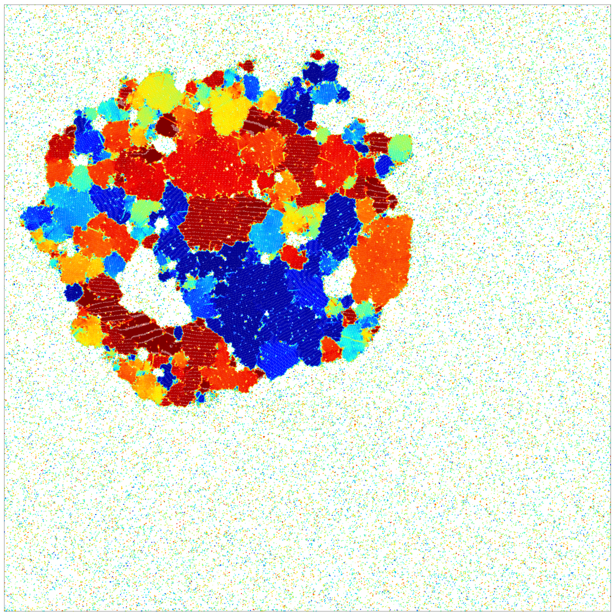

Dense/dilute separation[1]

For low packing fraction ϕ

a single round droplet

Growth[2,3] of a mosaic of

hexatic orders[2] with

gas bubbles[2,4,5] & defects[6]

[1] **Cates & Tailleur, Annu. Rev. Cond. Matt. Phys. 6, 219 (2015)**

[2] **Caporusso, Digregorio, Levis, LFC & Gonnella, PRL 125, 178004 (2020)**

[3] **Caporusso, LFC, Digregorio, Gonnella, Levis & Suma, in preparation**

[4] **Tjhung, Nardini & Cates, PRX 8, 031080 (2018)**

[5] **Shi, Fausti, Chaté, Nardini & Solon, PRL 125, 168001 (2020)**

[6] **Digregorio, Levis, LFC, Gonnella & Pagonabarraga, Soft Matter 18, 566 (2022)**

The growth law

Scaling of the structure factor and growth regimes

Different Pe

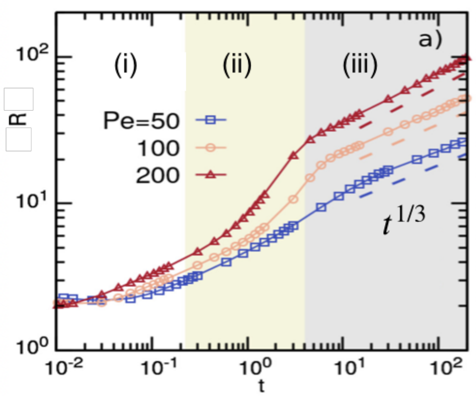

(i) nucleation (ii) condensation (iii) scaling

I peak:
system average
size

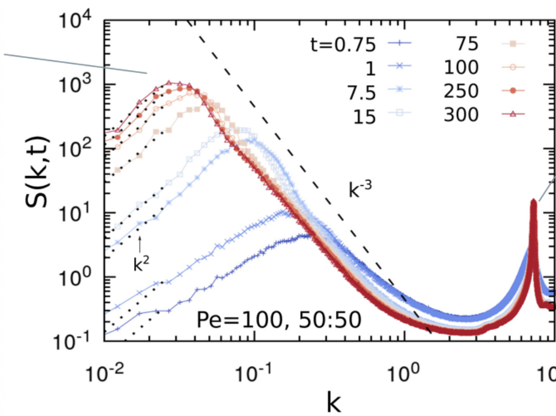

II peak:
particles' packing

$$S(\mathbf{k},t) = \sum_{i=1}^{N} e^{i\mathbf{k}(\mathbf{r}_i - \mathbf{r}_j)}$$

related to Fourier transform of
the pair correlation function

$$S(k,t) \sim R(t)^d\, f(kR(t))$$

In **scaling regime** $t^{1/3}$ like in **Lifshitz-Slyozov-Wagner**, scalar phase separation

The main subject of this talk

The coloured patches

Local hexatic order parameter : macro vs. micro

Crystalline patches

Orientational order

Local hexatic order parameter

$$\psi_{6j} = \frac{1}{nn_j} \sum_{k \in \partial_j} e^{i6\theta_{j,k}}$$

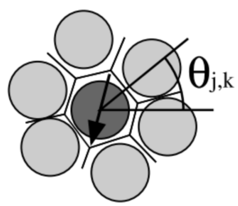

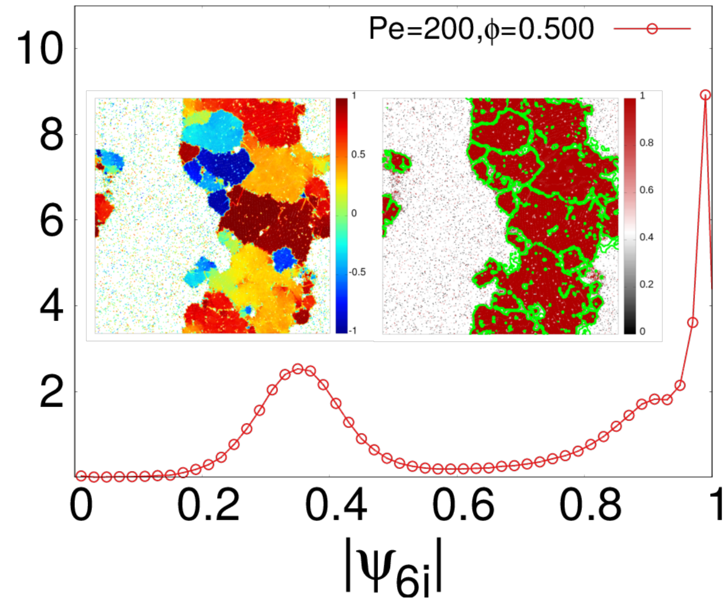

gas dense

Macro vs. Micro while $R(t) \to aL$ the hexatic saturates $R_H(t) \to R^s_H$ finite

— Approximately exponential distribution of hexatic cluster sizes

— Clusters of defects along the interfaces

Bubbles in cavitation

At the internal interfaces dynamic bubbles pop up

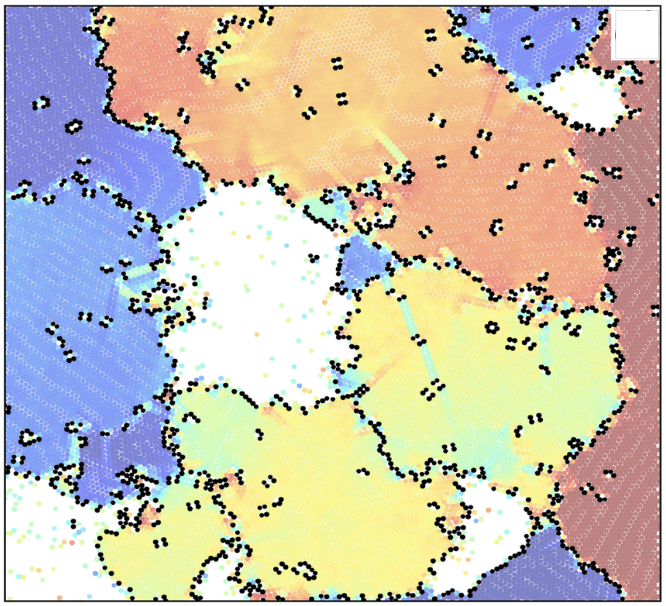

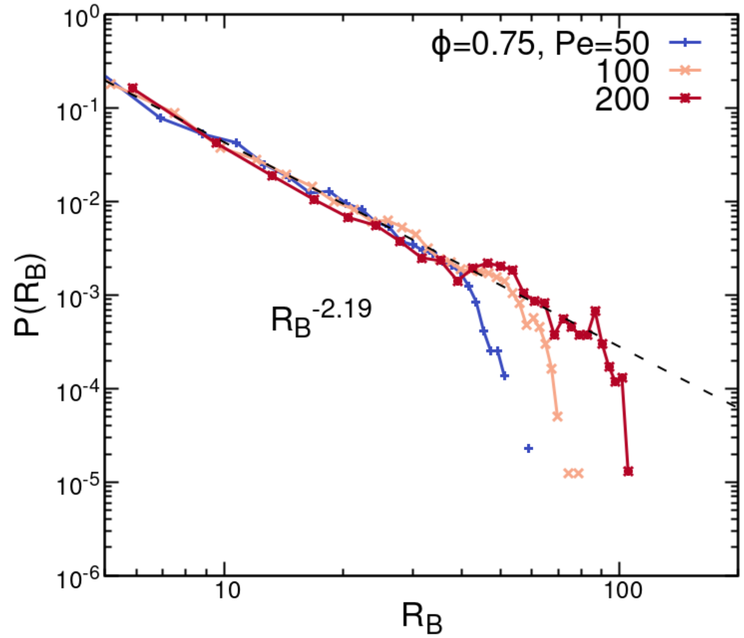

Bubbles appear and disappear at the interfaces between hexatic patches

Algebraic distribution of bubble sizes with a Pe-dependent exponential cut-off

Growth of dense components

Formation of dense clusters

Multinucleation, evaporation/coagulation, scaling regime, saturation

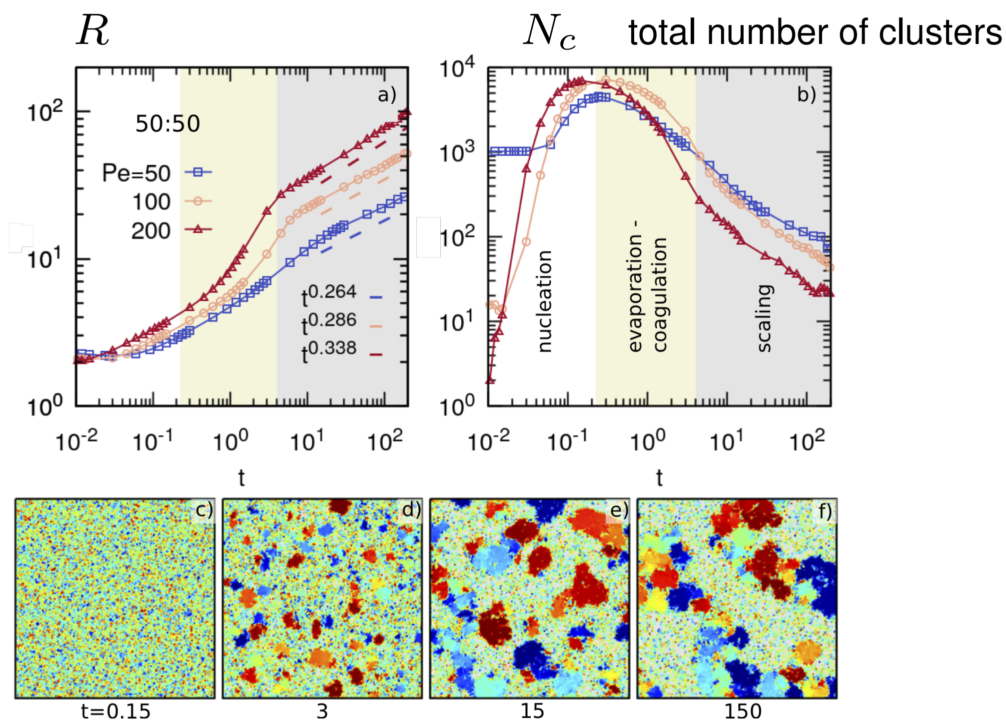

Nucleation Evap/coag Scaling

On the averaged scaling regime:

Redner, Hagan & Baskaran, PRL 110, 055701 (2013)

Stenhammar, Marenduzzo, Allen & Cates, Soft Matter 10, 1489 (2014)

Caporusso, Digregorio, Levis, LFC & Gonnella, PRL 125, 178004 (2020)

Beyond ?

Goals :

better understand the **mechanisms** for the growth process

like the one undergone by a system of **passive attractive particles** ?

Dense clusters

Instantaneous configurations (DBSCAN)

Passive

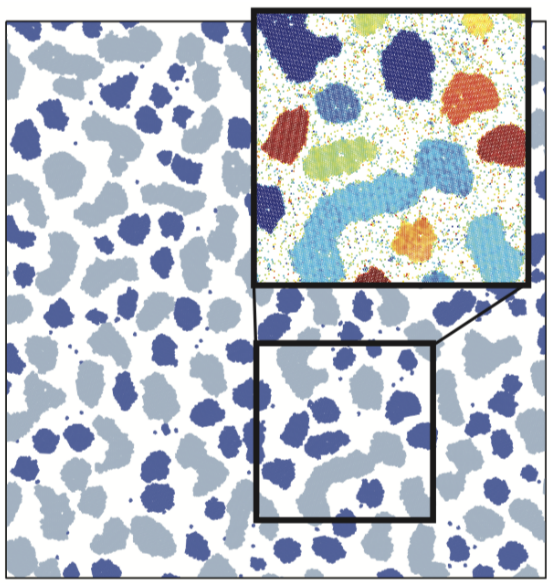

Active

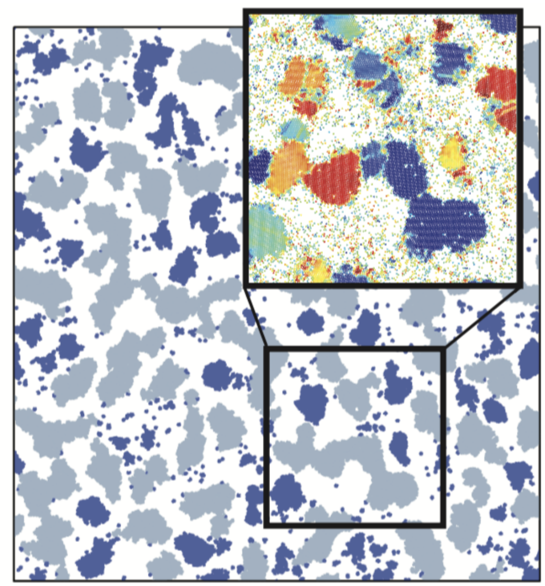

Parameters such that $R(t)$ is the same

Caporusso, LFC, Digregorio, Gonnella, Levis & Suma, soon in arXiv

Dense clusters

Visual facts about the instantaneous configurations

Similarities

- Large variety of shapes and sizes (masses)

  Co-existence of

  small regular (**dark blue**) and large elongated (**gray**) clusters

Differences

- Rougher interfaces in active
- Homogeneous (passive) vs. heterogeneous (active) orientational order

Dense active clusters

Instantaneous distribution of cluster masses

ABP clusters

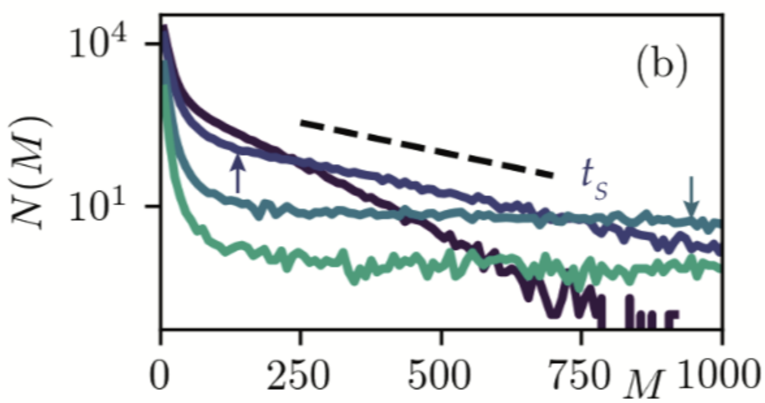

Curves at different times

Exponential at short t

Slow decay for $M > 200$

Janus particles

Ginot, Theurkauff, Detcheverry, Ybert & Cottin-Bizonne 18

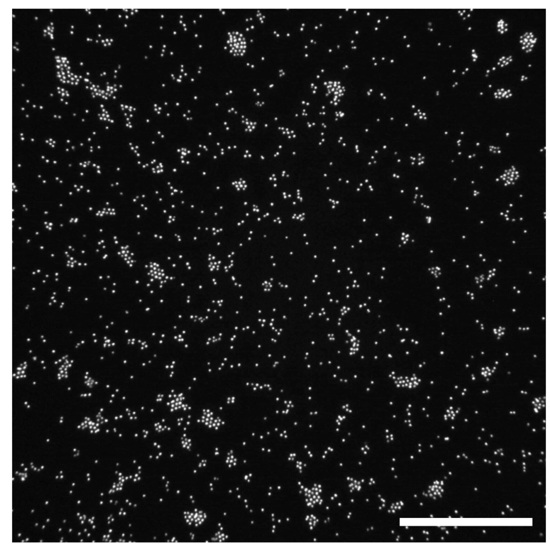

Smaller clusters than ours

Much lower ϕ and shorter t

Dense active clusters

Instantaneous distribution of cluster masses

ABP clusters

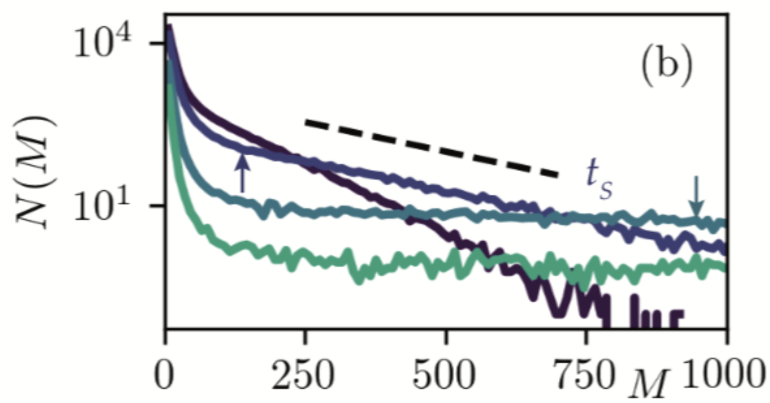

Curves at different times

Exponential at short t

Slow decay for $M > 200$

In the scaling regime

More structure to study

Janus particles

Ginot, Theurkauff, Detcheverry,

Ybert & Cottin-Bizonne 18

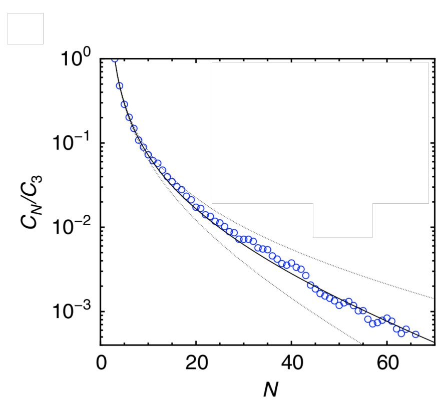

Similar exponential

up to $M \sim 60$

Smaller clusters than ours

Much lower ϕ and shorter t

Formation of dense clusters

Ostwald ripening vs. cluster-cluster aggregation - videos

Passive

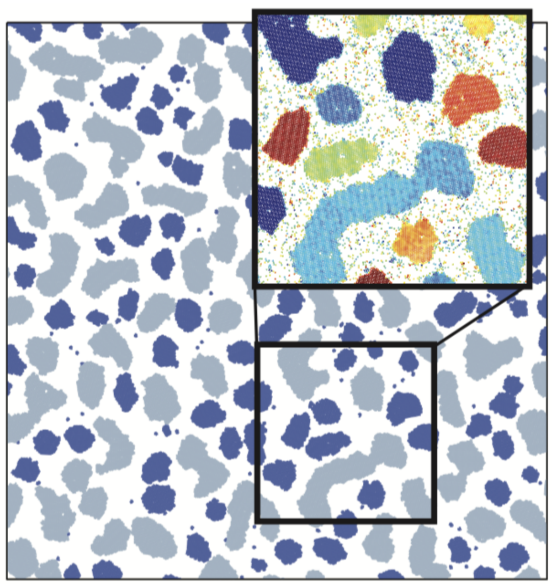

Active

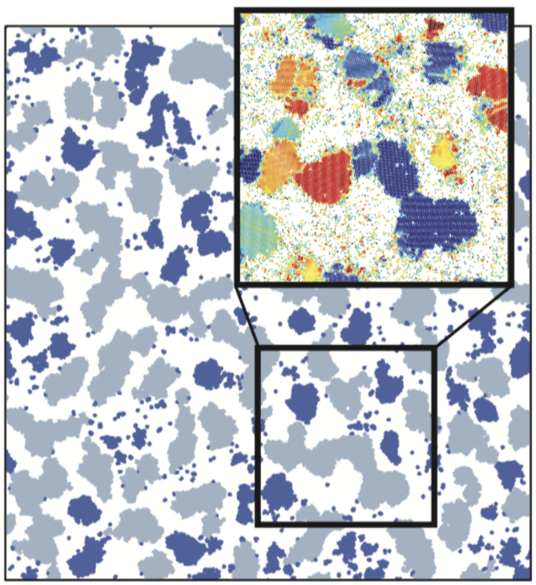

Dense clusters

Visual facts about the cluster dynamics

In both cases, **Ostwald ripening** features

- small clusters evaporate
- gas particles attach to large clusters

In the **active system**

- clusters displace much more & sometimes aggregate
- they also break & recombine

like in **diffusion limited cluster-cluster aggregation**

Cluster dynamics

Tracking of individual cluster motion - video

Active

Passive

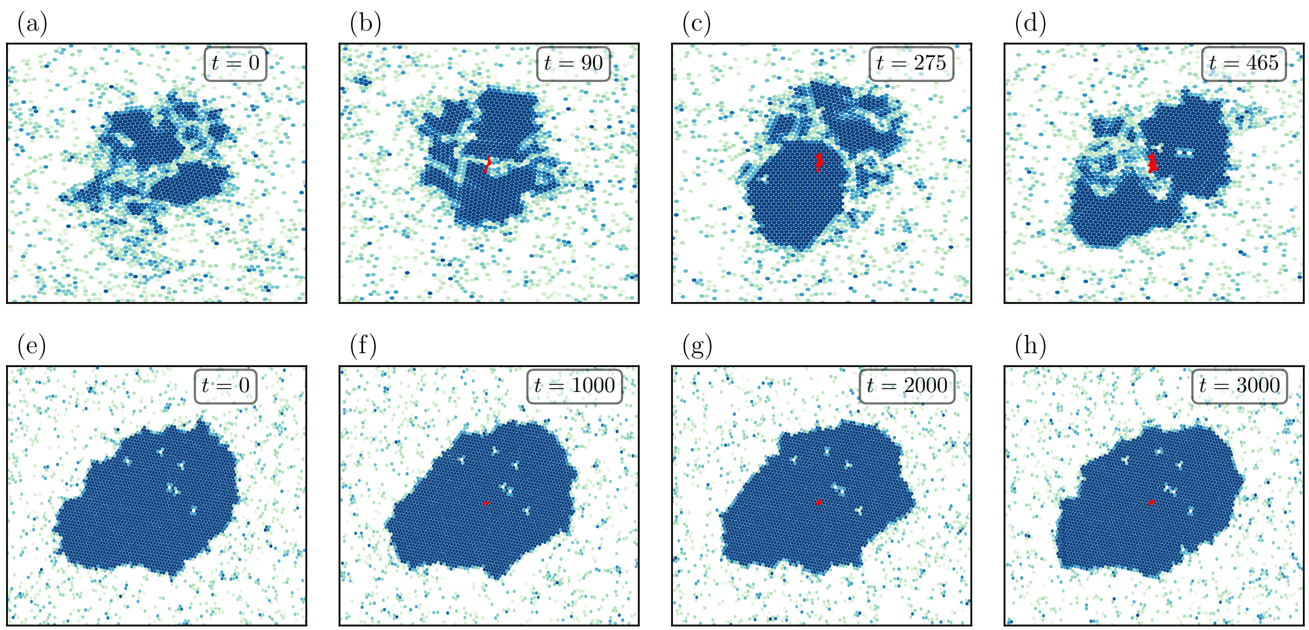

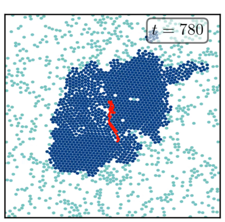

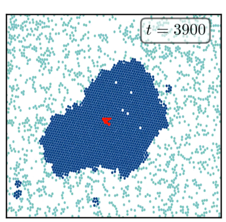

Active is much faster than passive

Cluster dynamics

Tracking of individual cluster motion – mass - time maps

Non-trivial numerical task:

identify and follow each cluster in the bulk

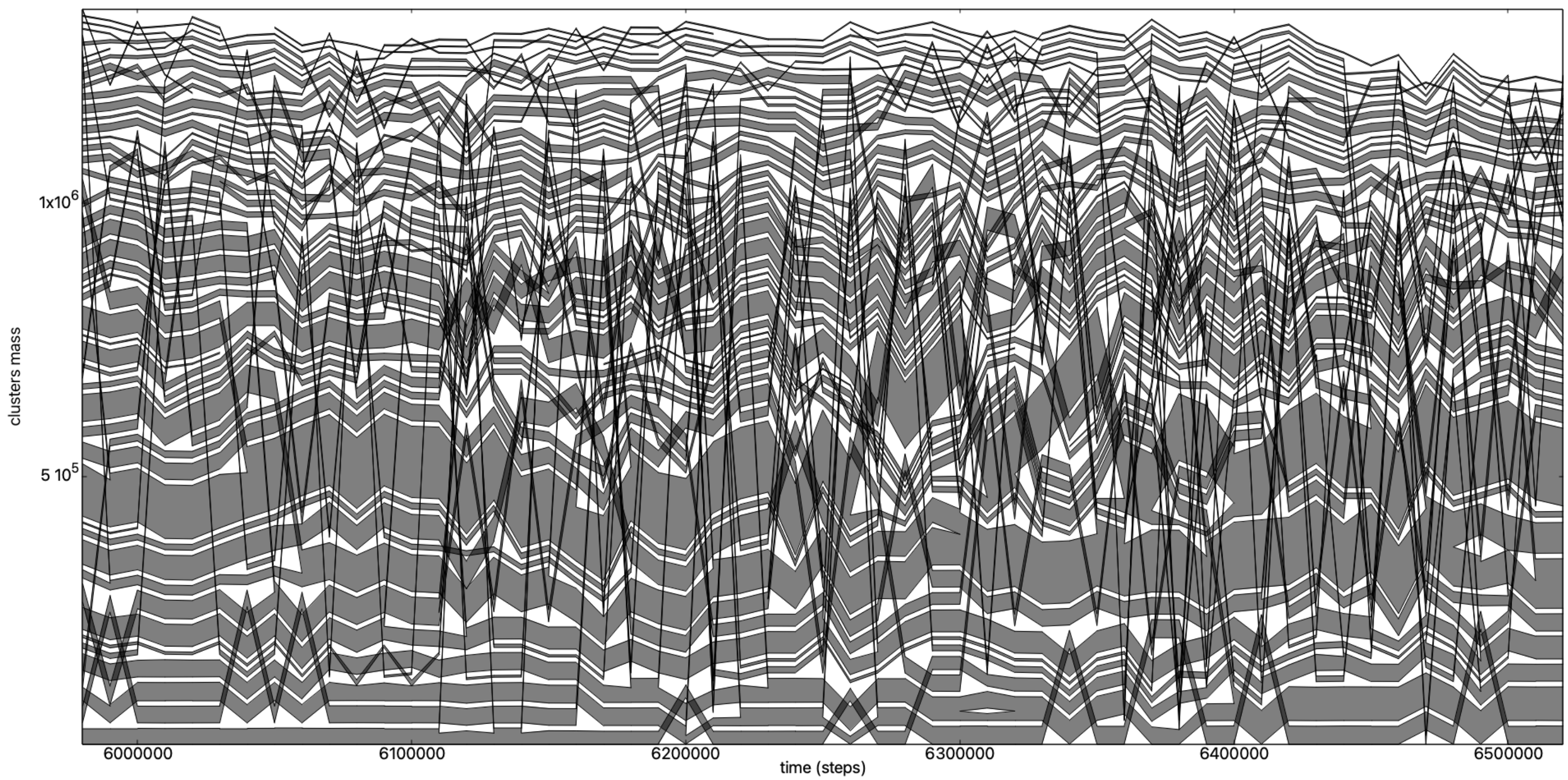

Caporusso, LFC, Digregorio, Gonnella, Levis, Suma, soon in arXiv

Cluster dynamics

Tracking of individual cluster motion – averaged cluster mass

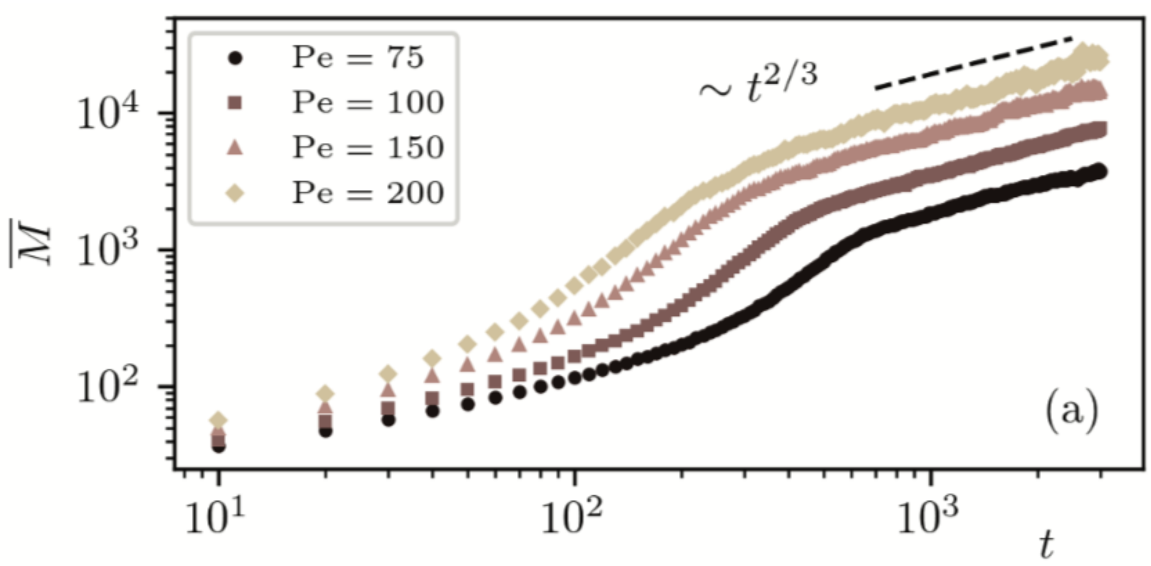

$$\overline{M}(t) \sim t^{2/3}$$

Cluster dynamics

Tracking of individual cluster motion

Non-trivial numerical task:

identify and follow each cluster in the bulk

Caporusso, LFC, Digregorio, Gonnella, Levis, Suma, soon in arXiv

Forces

- Total active force correlations $\langle \boldsymbol{F}(t) \cdot \boldsymbol{F}(0) \rangle = F^2 \, e^{-t/\tau_p}$
  with $F^2 \propto (M/m) F_{\rm act}^2$ and single particle τ_p
- Very weak torque

Evolution

- Enhanced diffusion, center of mass mean square displacement
  $\Delta^2 \Rightarrow D(M, \mathrm{Pe}) \sim M^{-\alpha} \, \mathrm{Pe}^2$ with $\alpha \sim 1/2$
- No rotational motion

Active cluster evolution

Averaged long times c.o.m. mean square displacement

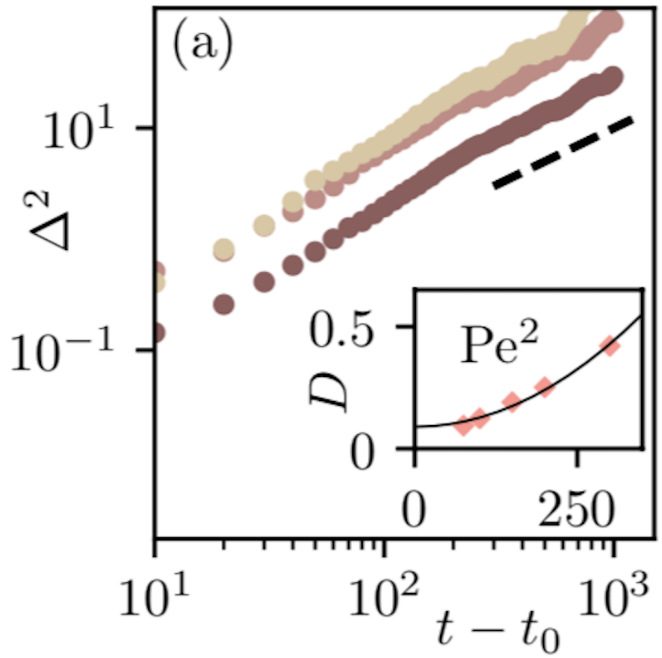

$$\Delta^2(t, t_0) = \frac{1}{N_c} \sum_{k=1}^{N_c} [\mathbf{r}^{(k)}_{\mathrm{c.o.m.}}(t) - \mathbf{r}^{(k)}_{\mathrm{c.o.m.}}(t_0)]^2 \sim 2d\, D(\mathrm{Pe})\, (t - t_0)$$

with the global diffusion coefficient $D(\mathrm{Pe}) \propto \mathrm{Pe}^2$

Fixed ϕ

Active cluster evolution

Enhanced diffusion : mass dependence of D

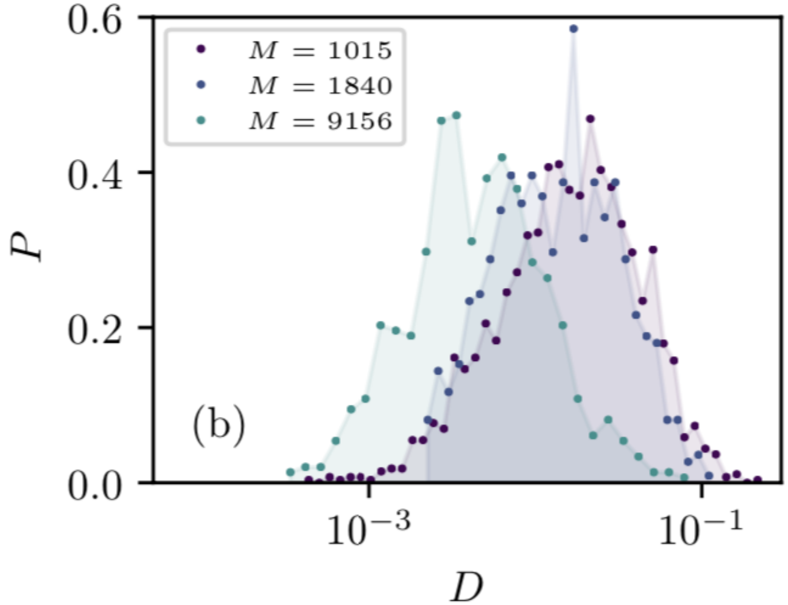

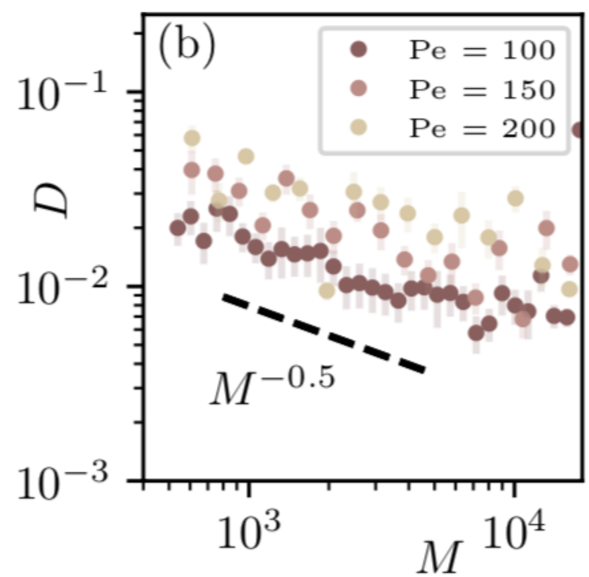

$$\Delta_k^2(t, t_0) = [\mathbf{r}^{(k)}_{\text{c.o.m.}}(t) - \mathbf{r}^{(k)}_{\text{c.o.m.}}(t_0)]^2 \sim 2d\, D(M_k, \mathrm{Pe})\,(t - t_0)$$

with the mass dependent diffusion coefficient $\boxed{D(M, \mathrm{Pe}) \sim M^{-1/2}\, \mathrm{Pe}^2}$

A sum of random forces yields M^{-1}

Active cluster evolution

Enhanced diffusion: mass dependence of D

Clusters extracted from the bulk

Passive active active **passive active active**

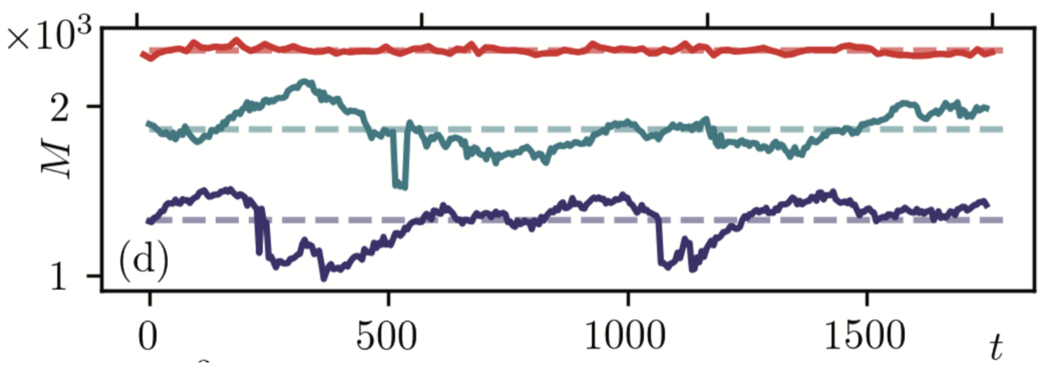

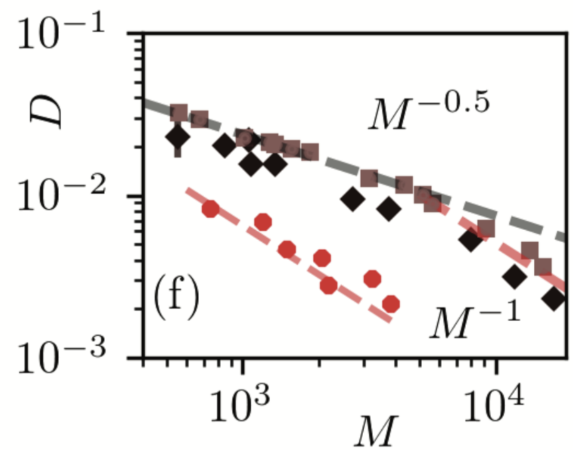

$$\Delta_k^2(t, t_0) = [\mathbf{r}^{(k)}_{\text{c.o.m.}}(t) - \mathbf{r}^{(k)}_{\text{c.o.m.}}(t_0)]^2 \sim 2d\, D(M_k, \text{Pe})\, (t - t_0)$$

Passive & very heavy active behave as $D \sim M^{-1}$

Extracted clusters

Enhanced diffusion: mass dependence of D

Clusters extracted from the bulk

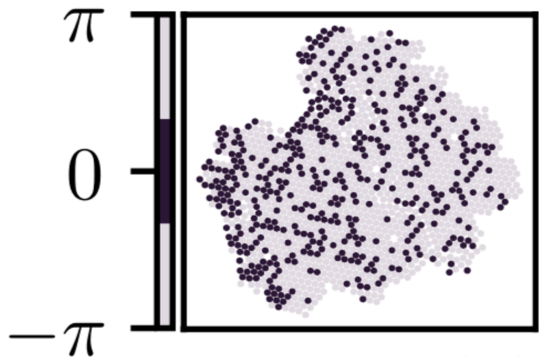

passive **active** **active**

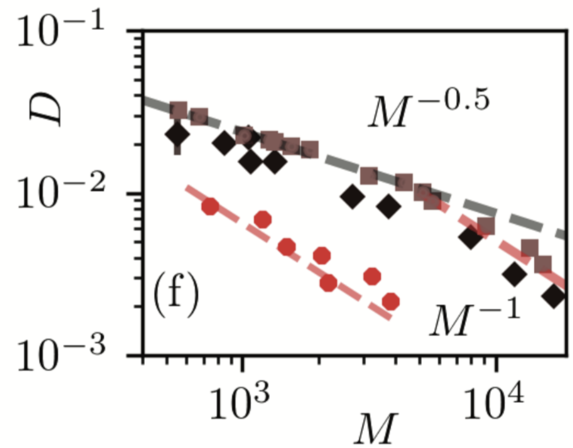

Local active force alignment

with direction of motion

$$D(M, \mathrm{Pe}) \sim M^{-\alpha}\,\mathrm{Pe}^2$$

Passive & very heavy active clusters behave as $D \sim M^{-1}$

Interpretation: surface effects lose importance

Geometry

Scatter plots: small regular – large fractal

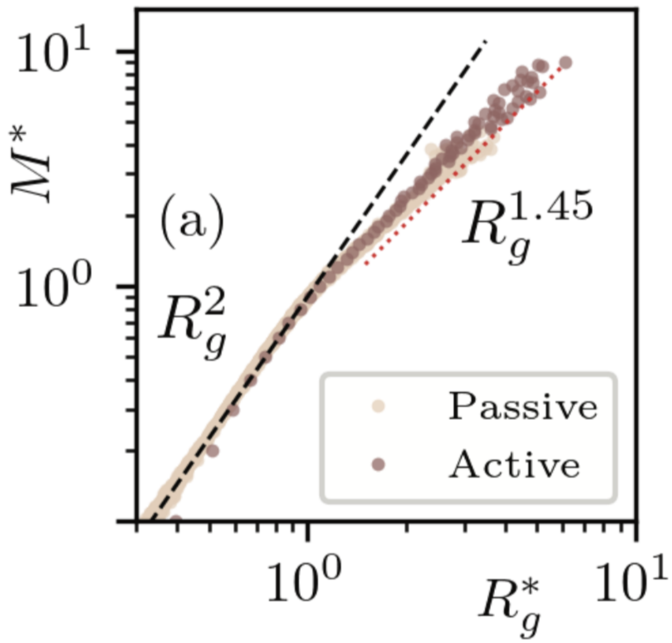

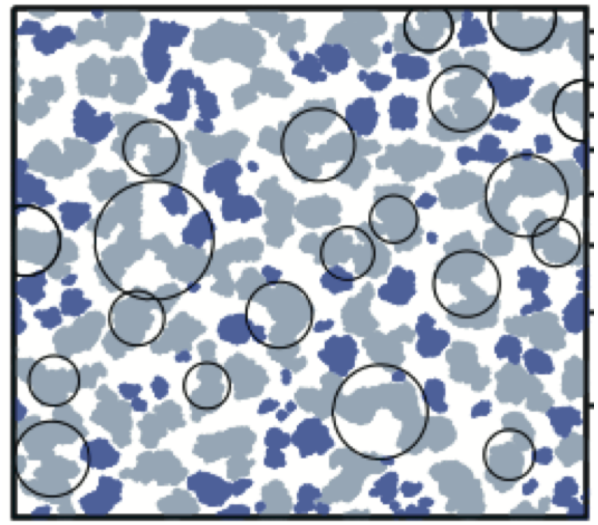

Cluster mass $M^*(t) = \dfrac{M_k(t)}{\overline{M}(t)}$ Gyration radius $R_g^*(t) = \dfrac{R_{g_k}(t)}{\overline{R_g}(t)}$

Data sampled in the scaling regime $t = 10^3 - 10^5$ every 10^3 time steps

$\overline{M}(t) = \dfrac{1}{N_c(t)} \sum_{k=1}^{N_c(t)} M_k(t)$ and $N_c(t)$ the total number of clusters at time t

Geometry

Scatter plots : small regular – large fractal

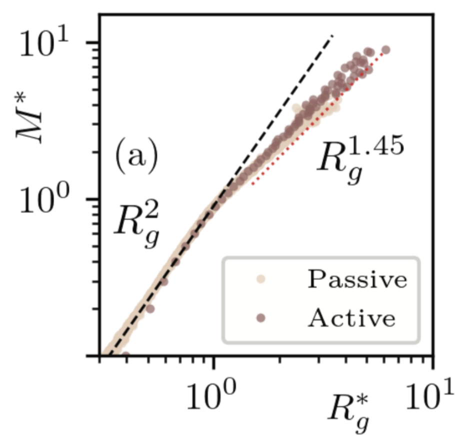

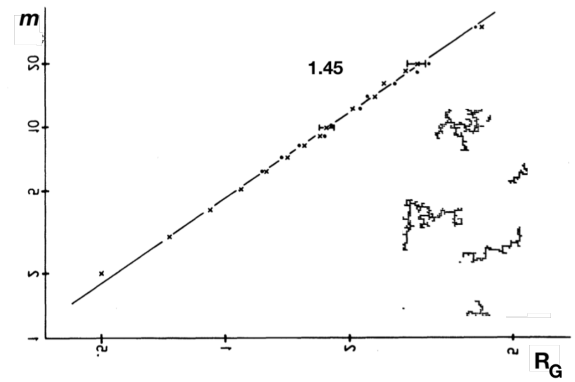

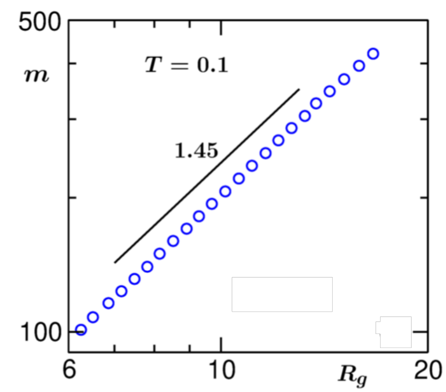

The ABP system

Caporusso et al. 22

Diffusion limited cluster-cluster aggregation

Kolb, Botet & Jullien, PRL 51, 1123 (1983)

Passive Lennard-Jones

Paul, Bera & S. K. Das, Soft Matter 17, 645 (2021)

Fractal dimension $d_f \sim 1.45$

holes of all sizes (algebraic pdf) – bubbles

elongated form

Cluster-cluster aggregation

Extended Smoluchowski argument

From $\overline{R}_g \sim t^{1/z}$ and using $D(M) \sim M^{-\alpha}$

Smoluchowski eq. $\Rightarrow z = d_f(1+\alpha) - (d - d_w)$

Regular clusters $M < M^*$

$d_f = d = d_w = 2$

$\alpha = 0.5$

$z = 2(1+0.5) = 3$

Fractal clusters $M > M^*$

$d_f = 1.45, d = 2$ and $d_w \sim 2$

$\alpha = 0.5$ in the bulk

$z = 1.45(1+0.5) = 2.18 < 3$

Reviews on the application of fractals to colloidal aggregation

R. Jullien, Croatia Chemica Acta 65, 215 (1992) P. Meakin, Physica Scripta 46, 295 (1992)

Regular vs fractal clusters

Radius of gyration and number

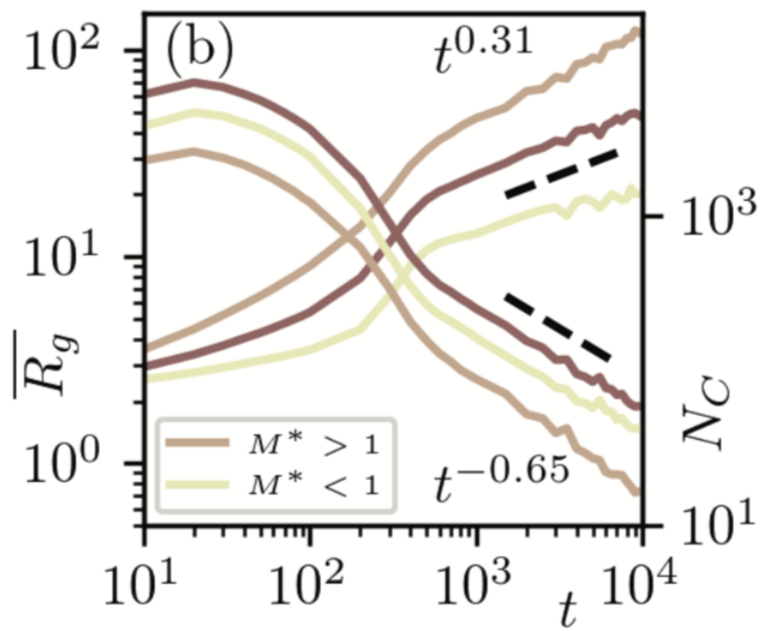

regular $z \gtrsim 3$ **fractal** $z \lesssim 3$ **average** $z = 1/0.31 \sim 3$

Cluster-cluster aggregation

Extended Smoluchowski argument

From $\overline{R}_g \sim t^{1/z}$ and using $D(M) \sim M^{-\alpha}$

Smoluchowski eq. $\Rightarrow z = d_f(1+\alpha) - (d - d_w)$

Regular clusters $M < M^*$

$d_f = d = d_w = 2$

$\alpha = 0.5$

$z = 2(1+0.5) = 3$

Fractal clusters $M > M^*$

$d_f = 1.45, d = 2$ and $d_w \sim 2$

if, instead, $\boxed{\alpha = 1}$

$z = 1.45(1+1) \sim 3$

Reviews on the application of fractals to colloidal aggregation

R. Jullien, Croatia Chemica Acta 65, 215 (1992) P. Meakin, Physica Scripta 46, 295 (1992)

Extracted clusters

Recall mass dependence of the diffusion coefficient

Cluster extracted from the bulk and set in contact with the same active gas

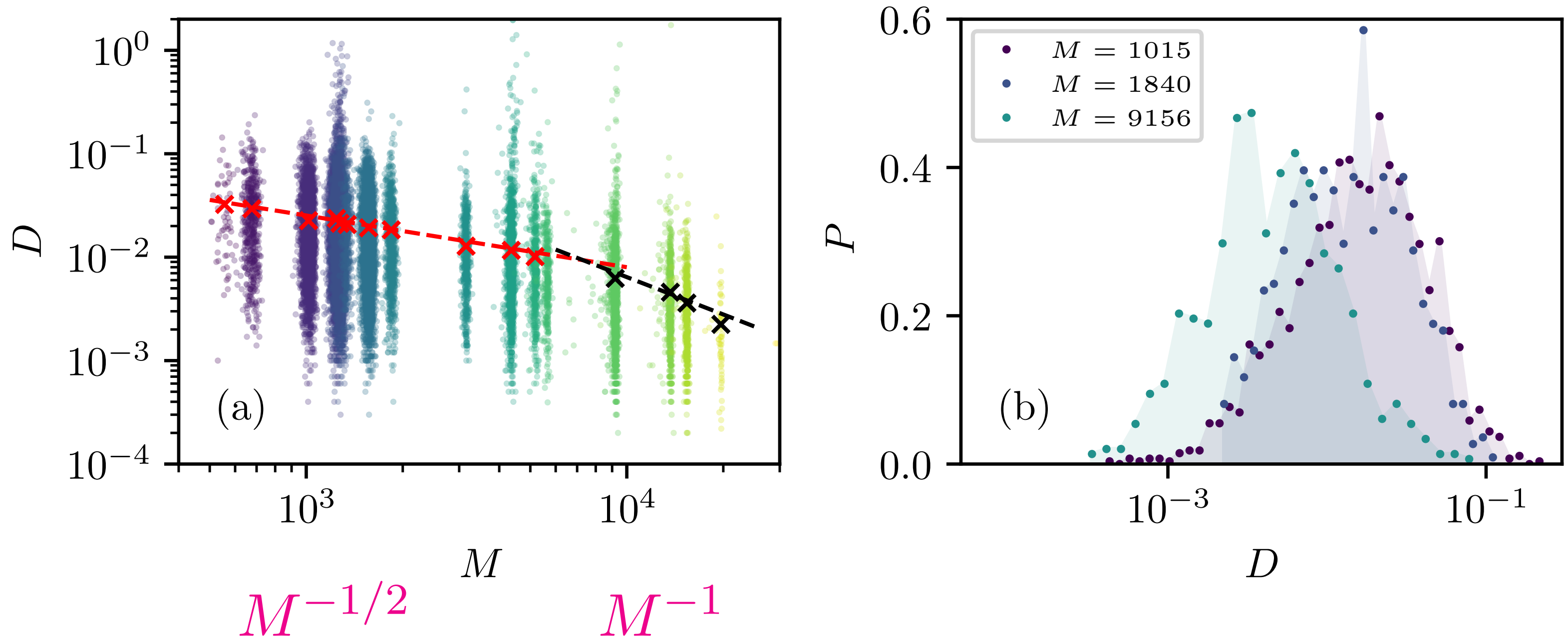

The very large ones cross over to $D \sim M^{-1}$ **at** $M \sim \overline{M}$

Interpretation: surface effects lose importance

Results I

We established the full

phase diagram of ABPs

solid, **hexatic**, **liquid** & **MIPS**

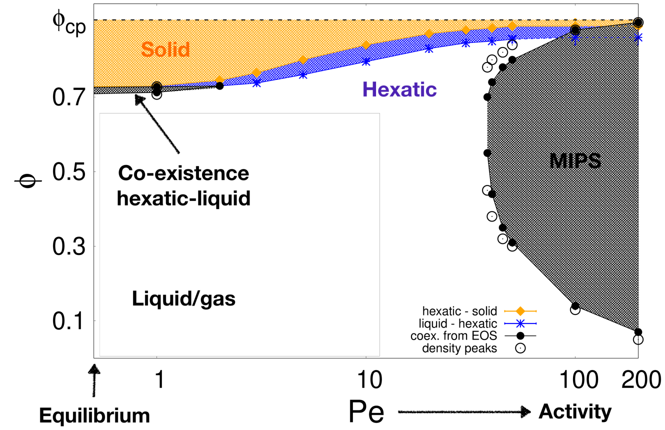

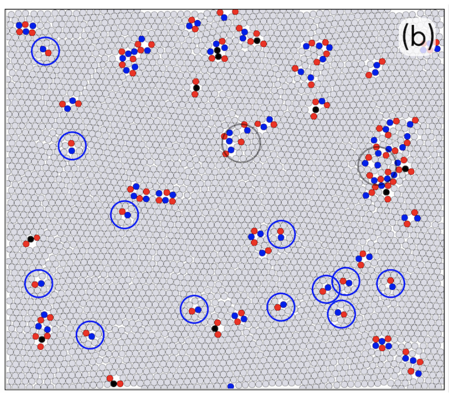

We clarified the role played by point-like

(**dislocations** & **disclinations**)

and **clustered** defects in

passive & active $2d$ models.

In **MIPS**

Micro *vs.* macro : hexatic patches & bubbles

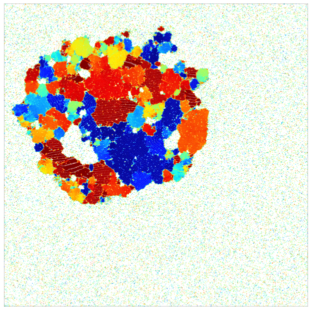

Results II

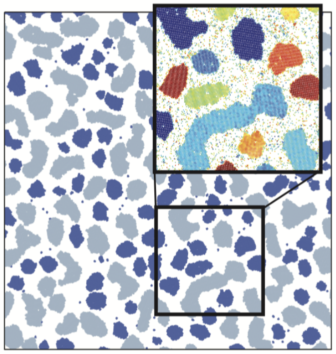

Difference between

Passive

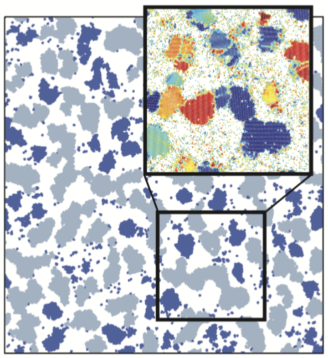

Active

growth

Ostwald ripening & cluster-cluster aggregation in active case
cluster-cluster aggregation almost not present in passive

Co-existence of regular and fractal clusters

Heterogeneous orientational order in large active clusters

Beyond disks

Phase diagrams & plenty of interesting facts

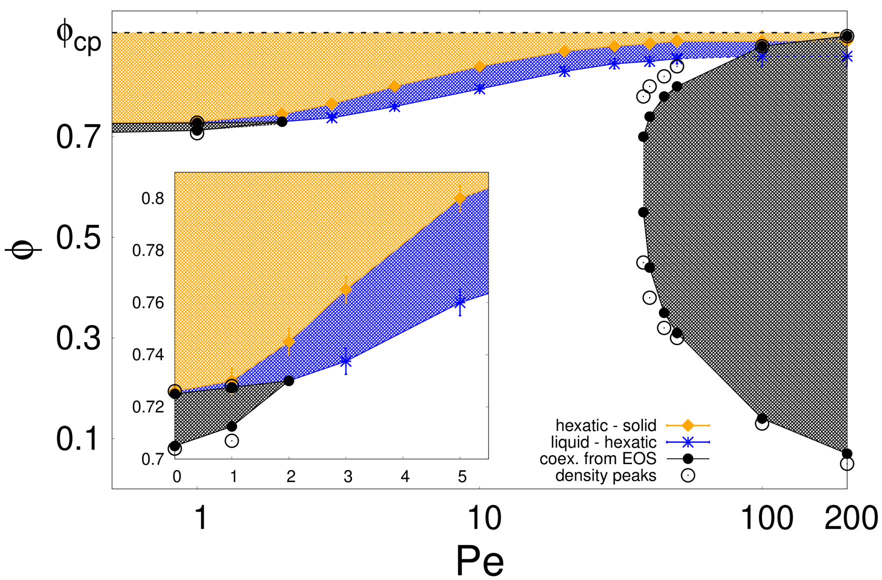

Disks

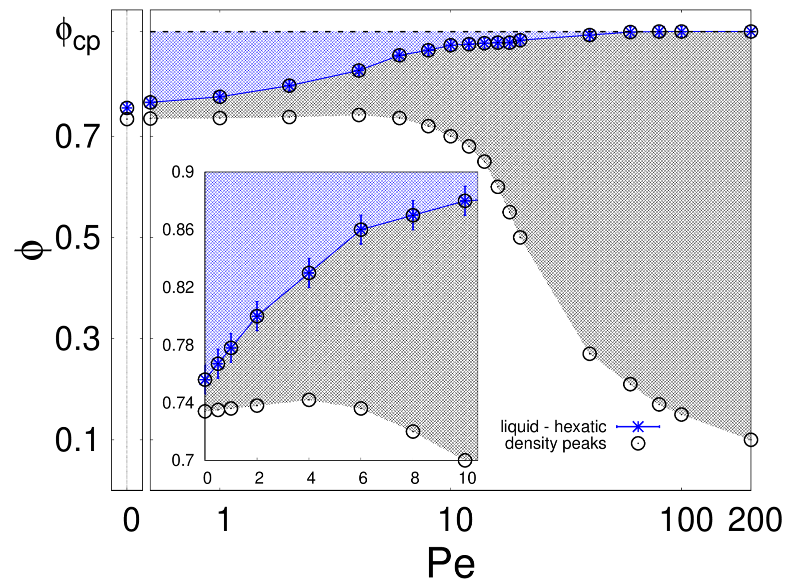

Dumbbells

Active dumbbells

Phase separating dynamics

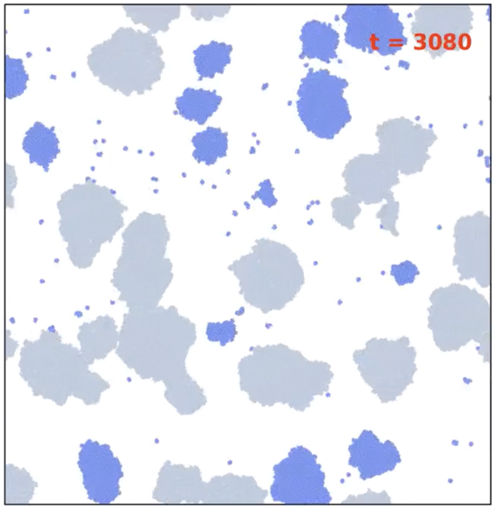

$2d$ Ising Model

Kawasaki dynamics – growing length & dynamic exponent

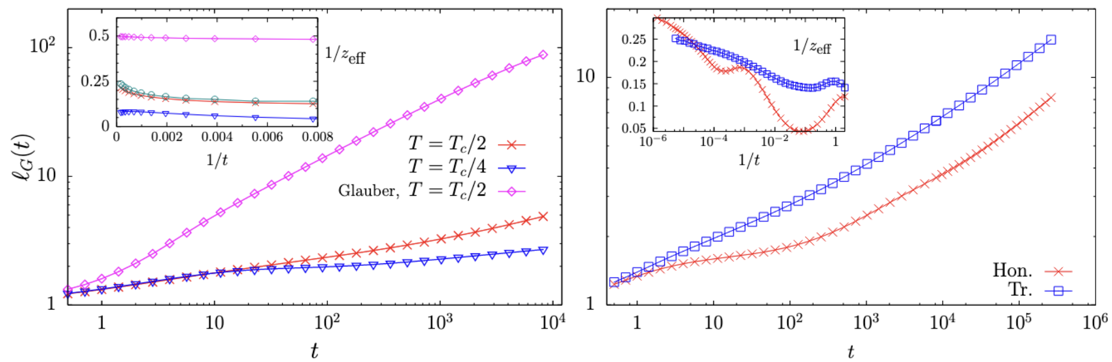

Figure 6: Local Kawasaki dynamics of the $2d$IM with balanced densities of the two species. The excess-energy growing length $\ell_G(t) = 1/\epsilon(t)$ against time following a sudden quench. Left panel: model defined on a square lattice with linear size $L = 640$ quenched to $T = T_c/2$ (red curve) and $T = T_c/4$ (blue curve) and, for comparison, data for NCOP dynamics at $T_c/2$ (purple curve). Right panel: growing length for Kawasaki dynamics on honeycomb and triangular lattices, with linear size $L = 320$, quenched to $T_c/2$. In the insets, we show the effective growth exponent, $1/z_{\rm eff}(t)$, computed as the logarithmic derivative of the function $\ell_G(t)$, plotted as a function of $1/t$. In the inset of the left panel, we also include the effective growth exponent estimated from the scaling of $\langle \theta^2 \rangle$ (circles).

$2d$ Ising Model

Kawasaki dynamics - scatter plot & fractal dimension

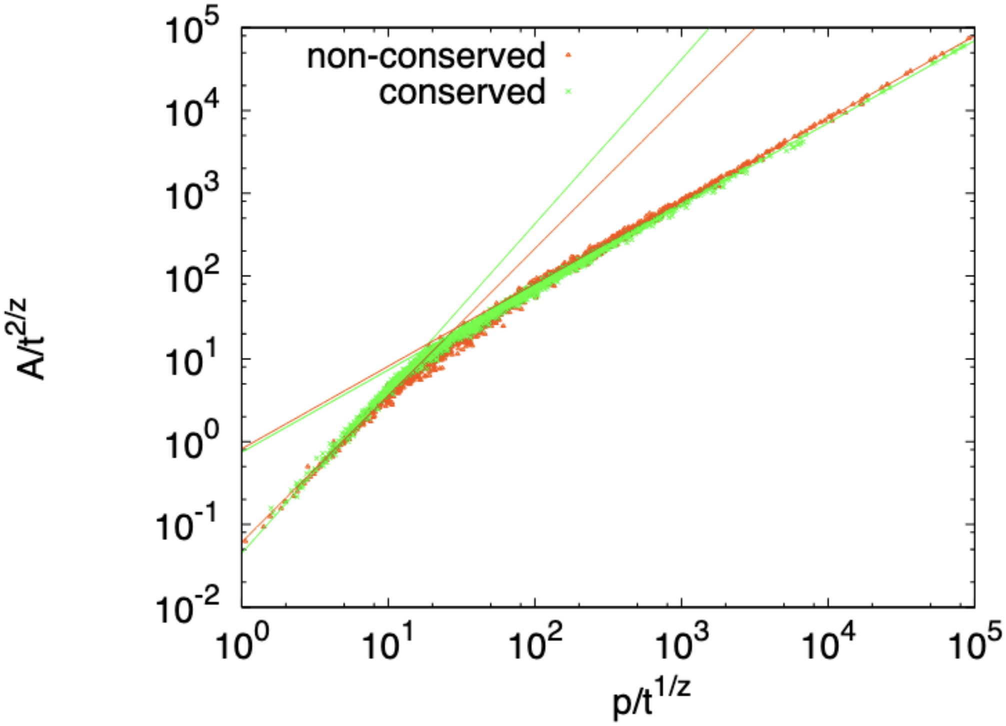

Topological defects

Summary of results

- **Solid** - **hexatic** à la BKT-HNY even quantitatively (ν value) and independently of the activity (Pe) $\boxed{\textit{Universality}}$

- **Hexatic** - **liquid** very few disclinations and not even free.

  $\boxed{\textit{Breakdown of the BKT-HNY picture for all Pe (even zero)}}$

- Close to, but in the liquid, $\boxed{\textbf{percolation} \text{ of } \textit{clusters of defects}}$ with properties of uncorrelated critical percolation (d_{f}, τ)

- In **MIPS**, network of defects on top of the interfaces between hexatically ordered regions, interrupted by the *gas bubbles in cavitation*

Cluster dynamics

Tracking of individual cluster motion

Non-trivial numerical task: **identify and follow each cluster**

Effective Active Brownian center of mass evolution ?

- Total active force correlations $\langle \mathbf{U}_{\rm a}(t) \cdot \mathbf{U}_{\rm a}(0) \rangle \Rightarrow \tau_p$
- Center of mass mean square disp $\Delta^2 \Rightarrow D(m_c, {\rm Pe}) \sim m_c^{-\alpha} {\rm Pe}^2$
- No rotational motion $\sim$ vanishing torque

Smoluchowski description of the $R \sim t^{1/z}$ with $z = 3$ growth ?

- Regular and fractal geometry $m_c = {R_{G_c}}^{d_f}$
- Cluster-cluster aggregation $z = d_f(1+\alpha) - (d - d_w)$

  d_w dimension of trajectory

Caporusso, LFC, Digregorio, Gonnella, Levis & Suma work in progress

Extracted clusters

Enhanced diffusion: mass dependence of D

Cluster extracted from the bulk and set in contact with the same active gas

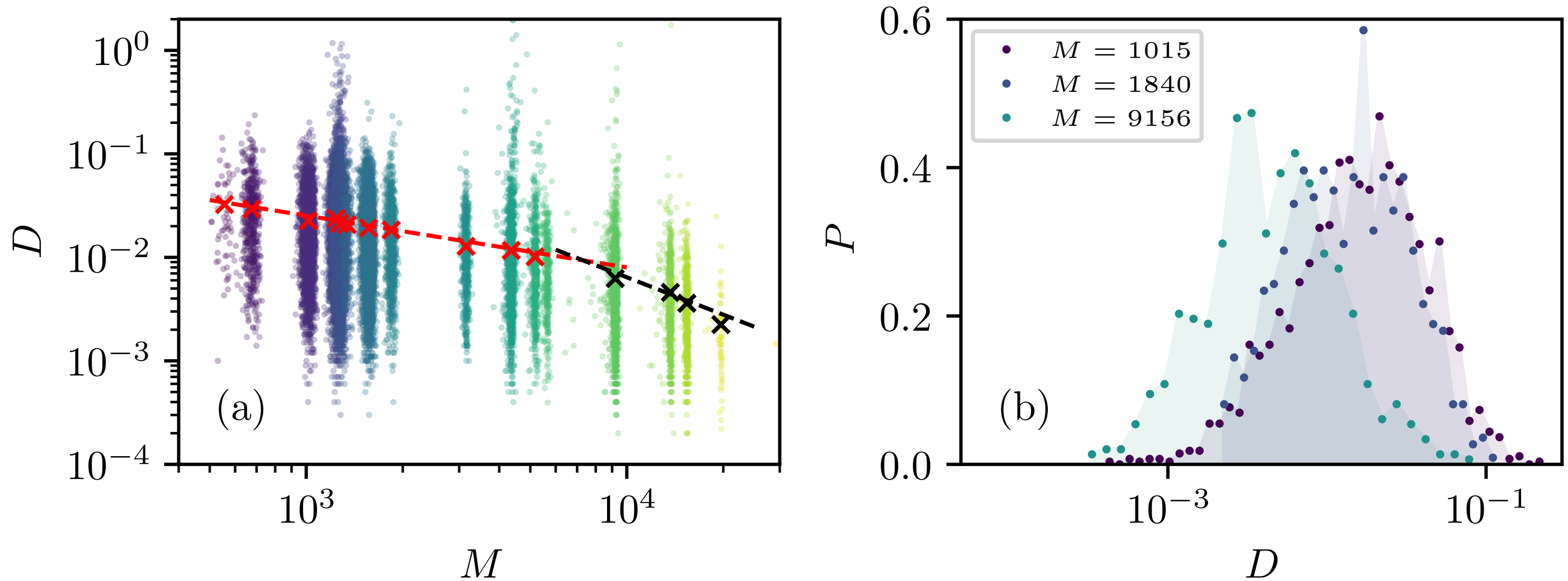

$M^{-1/2}$ M^{-1}

The very large ones cross over to $D \sim M^{-1}$ at $M \sim \overline{M}$

Interpretation: surface effects lose importance